# Realtime parallel back-projection algorithm for three-dimensional optoacoustic imaging devices

Ali Ozbek, X L Dean-Ben and Daniel Razansky\*

Institute for Biological and Medical Imaging, Technical University of Munich and Helmholtz Center Munich, Ingolstädter Landstrasse 1, 85764 Neuherberg, Germany.

#### ABSTRACT

Back-projection algorithms are probably the fastest approach to reconstruct an image from a set of optoacoustic (photoacoustic) data set. However, standard implementations of back-projection formulae are still not adequate for real-time (greater than 5 frames per second) visualization of three-dimensional structures. This is due to the fact that the number of voxels one needs to reconstruct in three-dimensions is orders of magnitude larger than the number of pixels in two dimensions. Herein we describe a parallel implementation of optoacoustic signal processing and back-projection reconstruction in an attempt to achieve real-time visualization of structures with three-dimensional optoacoustic tomographic systems. For this purpose, the parallel computation power of a graphics processing unit (GPU) is utilized. The GPU is programmed with OpenCL, a programming language for heterogenous platforms. We showcase that with the implementation suggested in this work imaging at frame rates up to 50 high-resolution three-dimensional images per second is achievable.

**Keywords:** Optoacoustic tomography, photoacoustic tomography, parallel back-projection algorithm, GPU acceleration

### 1. INTRODUCTION

Optoacoustic imaging is emerging as a non-invasive modality providing optical contrast with high resolution for imaging depths beyond the optical diffusion limit.<sup>1</sup> The technology combines the advantages derived from the low scattering of ultrasound waves and the high sensitivity and specificity of light absorption within biological tissues. Then, as the scattering of sound in tissues is several orders of magnitude lower than that of photons, optoacoustics renders high ultrasonic resolution for imaging depths up to a few centimeters with high contrast stemming from light absorption.<sup>1</sup>

The optoacoustic effect is unique in a way that it allows to simultaneously excite a whole three-dimensional (volumetric) region by using a single interrogating laser pulse. Thereby, the time resolution of the imaging method is theoretically limited by the time-of-flight of the optoacoustically-generated signals from the object, i.e., on the order of several microseconds to several tens of microseconds. In practice, it is however the pulse repetition rate of the laser (typically several Hertz) what mostly limits the achievable time resolution. The feasibility of imaging at the pulse repetition rate of the excitation laser has recently been showcased by simultaneous acquisition of optoacoustic signals with an array of cylindrically-focused ultrasonic transducers.<sup>2</sup> Whereas high-resolution cross-sectional images are rendered in real time (10 Hz), the reconstructions are generally affected by out-of-plane artifacts and quantification errors due to wrong assumptions in two dimensional reconstruction algorithms.<sup>3</sup> More recently, the feasibility of volumetric imaging in real time has been reported<sup>4,5</sup>, opening new interesting prospects of the optoacoustic technology to image dynamic events. Three-dimensional reconstruction is however time consuming, even when using fast algorithms. Thereby, the acceleration of the reconstruction procedure becomes a critical issue to be able to visualize three dimensional structures in real-time.

*E-mail:	dr@tum.de	

Opto-Acoustic Methods and Applications, edited by Vasilis Ntziachristos, Charles P. Lin, Proc. of OSA Biomedical Optics-SPIE Vol. 8800, 880001 · © 2013 OSA-SPIE CCC code: 1605-7422/13/\$18 · doi: 10.1117/12.2033376

### 2. THEORY

The optical energy of the illuminating laser pulse is absorbed within biological tissues leading to a thermal expansion field proportional to the absorbed radiation. This induces a pressure field throughout the illuminated tissue. Since the duration of the laser pulse is in the order of nanoseconds, the thermal diffusion can be neglected. Under these circumstances, the temporal light intensity of the laser illumination can be expressed with a Dirac delta function  $\delta(t)$ . Thus, the resulting optoacoustic waves can be expressed with the following equation.

$$\frac{\partial^2 p(r,t)}{\partial t^2} - c^2 \Delta p(r,t) = \Gamma H(r,t) \frac{\partial \delta(t)}{\partial t}$$
 (1)

where r is the spatial location vector, t is time, c is the speed of sound in the homogenous medium,  $\Gamma$  is the Grüneisen parameter and H(r) is a scalar field which represents the energy absorbed in the tissue per unit volume. Poisson's solution to eq. 1 can be utilized to calculate the pressure field as follows

$$p(r,t) = \frac{\Gamma}{4\pi c} \frac{\partial}{\partial t} \int_{S'} \frac{H(r')}{|r-r'|} dS'$$
 (2)

where S' is the spherical, time dependent surface for which |r - r'| = ct. The purpose of optoacoustic reconstructions is to map the absorption field H(r') from the recorded acoustic signals. A numerical discretization and subsequent inversion of eq. 2 can be employed for an accurate optoacoustic reconstructions,<sup>6</sup> which is however generally slow. Assuming that the tissue is a homogenous medium, the field H(r') can also be estimated with a universal back-projection formula given by<sup>7</sup>

$$H(r') = \frac{1}{\Gamma} \int_{\Omega} \frac{d\Omega}{\Omega} \left[ 2p(r,t) - 2t \frac{\partial p(r,t)}{\partial t} \right] \Big|_{t = \frac{|r-r'|}{c}}$$
(3)

The constants in eq. 3 are omitted for simplicity. Furthermore, for a scanning radius much larger than the object, the equation 3 can be discretized as following<sup>8</sup>

$$H(r'_j) = \sum \left[ p(r_i, t_{ji}) - t_{ji} \frac{\partial p(r_i, t_{ji})}{\partial t} \right]$$
(4)

where  $r_i$  is the position of the *i*-th transducer,  $r'_j$  is the position of the *j*-th point of the reconstruction region of interest and  $t_{ji} = |r_i - r'_j|/c$ .

### 3. IMPLEMENTATION

In order to improve performance, eq. 4 can be simplified at the expense of reconstruction accuracy. Since the goal of this work is enabling real-time reconstruction, the accuracy loss is negligible for our purposes. The term p(r,t) in eq. 4 can be neglected with respect to the second term in the equation. Moreover, multiplication with t can also be omitted as in our region of interest (ROI) the change in t is below 10% which can also be neglected for our purposes. After these two simplifications, eq. 4 can be written as follows

$$H(r'_j) = \sum \left[ -\frac{\partial p(r_i, t_{ji})}{\partial t} \right] \tag{5}$$

Prior to the reconstruction, the recorded signal is also deconvolved with the impulse response of the ultrasonic transducers and band-pass filtered for noise reduction. The differentiation in eq. 5 can be implemented concurrently with the filtering and deconvolution. Thus, eq. 5 can be expressed as

$$H(r') = \sum p_{filt}(r'_i, t_{ji}) \tag{6}$$

where  $p_{filt}$  is the filtered acoustic signal which can be expressed as

$$p_{filt} = g(t) * p(t) \tag{7}$$

where p(t) is the raw acoustic signal data and g(t) is the impulse response of the filter. Since deconvolution is implemented as a Wiener filter, it can be combined with noise-reduction filtering and differentiation to create one custom filter g(t) which can be then written as following

$$g(t) = h_{noise} * h_{wiener} * \frac{\partial}{\partial t} \delta(t)$$
 (8)

where  $h_{noise}$  is impulse response of the noise-reduction filter,  $h_{wiener}$  is the Wiener deconvolution filter and  $\delta(t)$  is the Dirac-delta function. The reconstruction algorithm is implemented on the GPU in two parts. First the signal is pre-processed according to eq. 8. Then, the processed signal is reconstructed using the simplified reconstruction algorithm in eq. 6.

The GPU on which the reconstruction algorithm is run, was programmed with OpenCL. It is a framework for programming heterogenous platforms consisting (multi-core)CPUs and GPUs. With OpenCL it is possible to program GPUs for scientific calculations and harness its parallel processing capabilities. In OpenCL the parallelism is expressed with kernels. Kernels are functions which may execute in parallel or sequentially on any OpenCL compatible hardware such as GPUs and CPUs. When a kernel is executed, numerous instances of the kernels are launched. Each instance of the kernel is called a work item. The work items are grouped into work groups. Work groups enable data sharing and work item synchronization between work items within the same work group. Depending on the programming and hardware limitations, work items can be executed in parallel or sequentially.<sup>9</sup>

The convolution in eq. 7 is implemented as a sliding dot product. Filtering is done in the time domain instead of in the frequency domain. This allows the impulse response g(t) of our filter to be cropped, which reduces the number of steps in the calculation. A work item is launched for each instance of  $p_{filt}$ , calculating its value (Fig. 1).

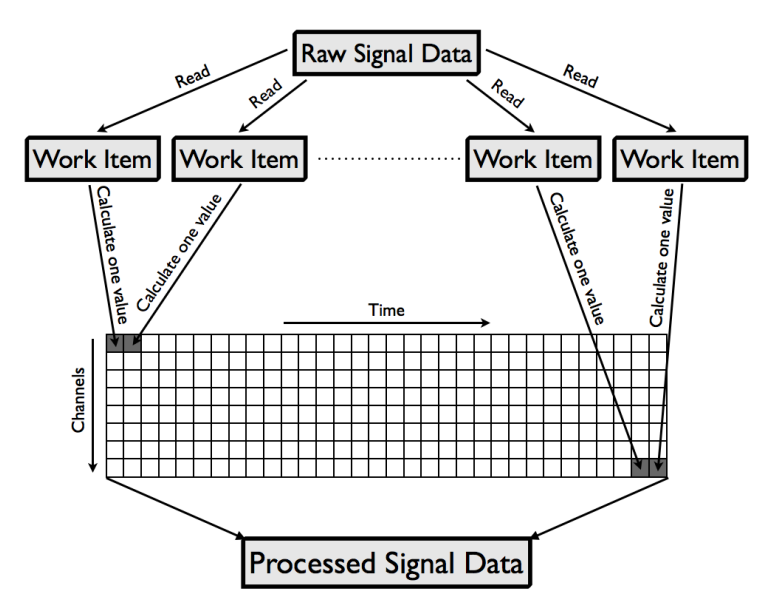


Figure 1. Work flow of the filtering process.

After filtering,  $p_{filt}$  is used to reconstruct a three-dimensional image using eq. 6. Similar to the filtering process, the value of each voxel H(r') is calculated with one work item 2. The summation in eq. 6 is done sequentially. This approach uses the computational resources of the GPU more efficiently in comparison to

calculating the summation in parallel. Parallel implementation of summation forces some of GPUs processing elements to idle which results in loss of performance.

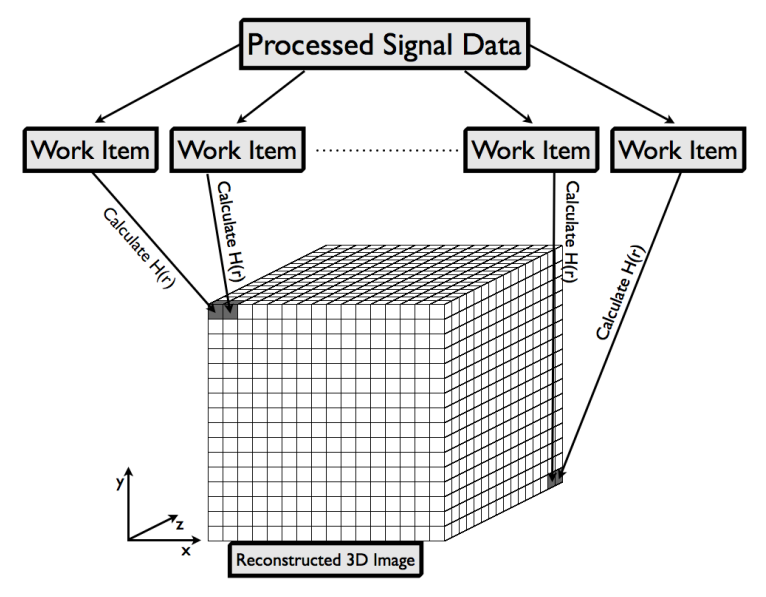


Figure 2. Work flow of the reconstruction.

## 4. RESULTS

In this work is an ATI HD 7970 general purpose GPU with 3GB of memory was used. It has 64 stream cores per compute unit and 32 compute units, which allows execution of 2048 work items in parallel.

During the tests a 128x128x64 3D image took 19.5 ms to reconstruct which corresponds to approximately 51 frames per second. When the constructed image was visualized with the MATLAB interface, the total frame rate dropped down to 35 frames per second. This is probably a result of MATLAB subroutines running during the visualization of the 3D image. Despite the performance loss caused by the MATLAB interface, the resulting frame rate is much faster than the reconstruction times on the CPU. A comparison of the performance of different processing element types is displayed in Figure 3.

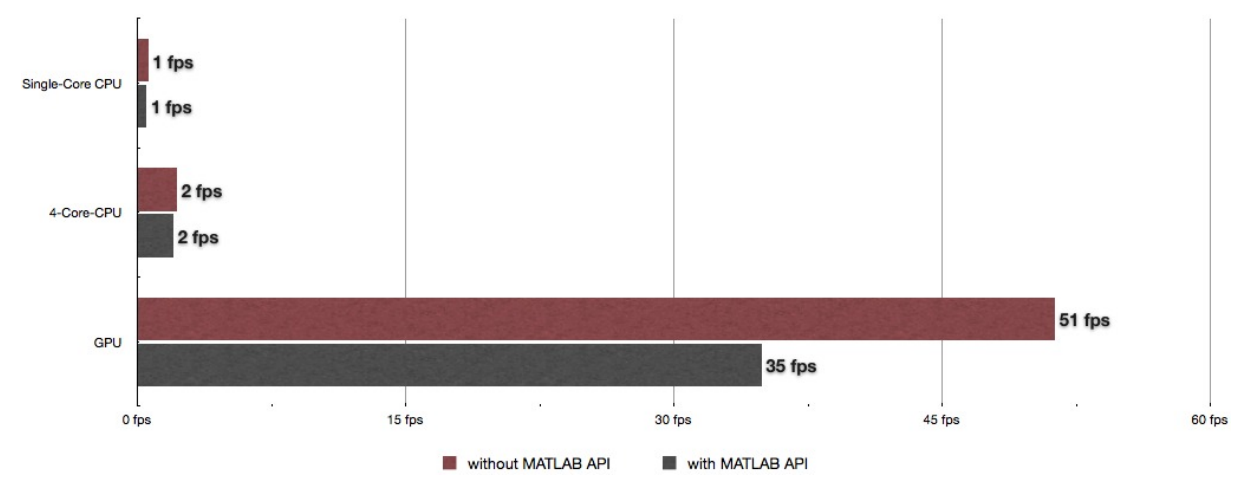


Figure 3. Performance comparison of different processing element types.

The relationship between resolution and computation time is represented in Figure 4. In the graph two distinct regions can be differentiated. In the left part where the reconstruction resolution is low, the reconstruction time

remains constant around 2 milliseconds. Here, the main limiting factor to the reconstruction is the data transfer times between the GPU and the CPU. After a certain limit is reached (in this case  $2^{14}$  voxels), the reconstruction time increases linearly with the number of voxels. In this right part of the graph the parallel processing capabilities of the GPU are exceeded and a portion of work items are executed sequentially. Thus the computation time becomes the dominant factor in determining the reconstruction time.

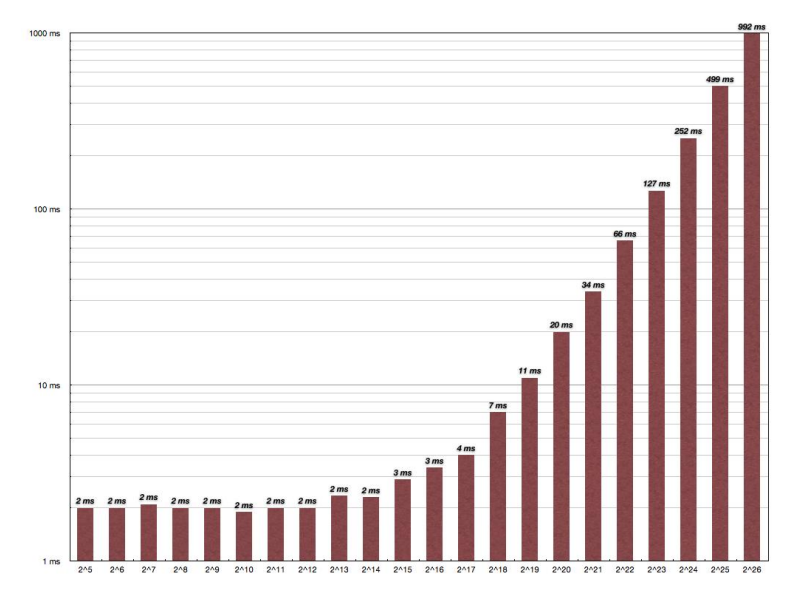


Figure 4. Relationship between number of reconstructed voxels and reconstruction time

## 5. CONCLUSIONS

In this work, we have successfully accelerated optoacoustic reconstructions to enable a real-time visualization of volumetric images with three-dimensional optoacoustic tomographic imaging systems. A parallelized version of the back-projection algorithm was implemented with OpenCL on an ATI HD 7900 series GPU, reaching up to 51 reconstructions per second with a resolution of 128x128x64. The back-projection reconstruction procedure also included a convenient implementation of a noise-reduction filtering, differentiation and deconvolution with the impulse response of the transducer.

## Acknowledgements

Daniel Razansky acknowledges support from the European Research Council under Starting Independent Researcher Grant ERC-SG-LS7 Dynamit.

### REFERENCES

- [1] Minghua Xu and Lihong V. Wang., "Photoacoustic imaging in biomedicine," Review of Scientific Instruments 77(4) 2006.
- [2] Buehler, A., Herzog, E., Razansky, D., and Ntziachristos, V., "Video rate optoacoustic tomography of mouse kidney perfusion," *Optics Letters* 35(14), 24752477 (2010).
- [3] Dean-Ben, X. L., Nziachristos, V., and Razansky, D., "Acceleration of optoacoustic model-based reconstruction using angular image discretization," *IEEE Transactions on medical imaging* 31(5), 11541162 (2012).
- [4] Buehler A., Den-Ben X. L., Claussen J., Ntziachristos V. and Razansky. D., "Three-dimensional optoacoustic tomography at video rate," *Optics Express* (20):20, 2012.
- [5] B Wang, L Xiang, M S Jiang, J Yang, Q Zhang, P R Carney, and H Jiang., "Photoacoustic tomography system for noninvasive real-time three-dimensional imaging of epilepsy," *Biomedical Optics Express*, 3(6):14271432, 2012.
- [6] Dean-Ben, X. L., Buehler, A., Ntziachristos, V., and Razansky, D., "Accurate model-based reconstruction algorithm for three-dimensional optoacoustic tomography," *IEEE Transactions on Medical Imaging* 31(10), 19221928 (2012).
- [7] Minghua Xu and Lihong V. Wang., "Universal back-projection algorithm for optoacoustic computed tomography," *Physical Review E* 71:016706 2005.
- [8] Dean-Ben, X. L., Ma, R., Razansky, D., and Ntziachristos, V., "Statistical approach for optoacoustic image reconstruction in the presence of strong acoustic heterogeneities," *IEEE Transactions on Medical Imaging* 30(2), 401408 (2011).
- [9] Khronos OpenCL Working Group, The OpenCL Specification 1.2, (2012).